LHCb-CONF-2015-001
March 12, 2015

Study of the decay $B^+ \to K^+\pi^0$ at LHCb

The LHCb collaboration [†]

Abstract

This analysis investigates the capability of LHCb to study the decay mode $B^+ \to K^+\pi^0$. This serves as a prototype analysis for decay channels with similar topologies, such as the $B^0 \to K^0_S\pi^0$, the $\Lambda^0_b \to \Lambda\gamma$, and the $B^0 \to K^0_S\pi^0\gamma$ decays, which involve photons in the final state and lack a reconstructed decay vertex. There is significant interest in these channels due to their sensitivity to effects of physics beyond the standard model. The proton-proton collision data set collected in 2011–2012, corresponding to 3.0 fb^{-1} of integrated luminosity, is studied. An analysis strategy is developed to mitigate the effects of low trigger efficiency and large combinatorial background leading to the reconstruction of 72 ± 26 signal events with a statistical significance of 3.7σ. Based on the findings of this study, a dedicated software trigger is being developed for use in the next data-taking period scheduled for later this year, when the LHC centre-of-mass energy will be increased.

LHCb-CONF-2015-001
13/03/2015

© CERN on behalf of the LHCb collaboration, license CC-BY-3.0.

[†]50th Rencontres de Moriond on Electroweak Interactions and Unified Theories, La Thuile, Italy, 14 - 21 March 2015. Contact author: J. E. Andrews, jea@umd.edu;

1 Motivation

Rare decays of heavy-flavoured hadrons that primarily proceed through hadronic or radiative penguin (loop) diagrams are amongst the most powerful probes for the effects of new physics beyond the Standard Model (SM). The polarisation of the photon in decays such as $B^0 \to K^0_S \pi^0 \gamma$, $B^0_s \to \phi\gamma$, and $\Lambda^0_b \to \Lambda\gamma$ can provide strong bounds on the effects of new physics. The family of $B \to K\pi$ decays, dominated by hadronic penguin amplitudes in the SM, can be influenced by the presence of additional amplitudes due to new physics. Measurements [1] in the $B \to K\pi$ decays at CDF, the B factories, and LHCb, have revealed significant deviations from the expected pattern of CP-violating asymmetries in these channels, the so-called "$K\pi$ puzzle". While LHCb has already improved the measurements in the $B^0 \to K^+\pi^-$ decay [2], a resolution of the puzzle requires a comprehensive study of the entire decay family, including improved measurements of final states containing π^0 mesons.

The LHCb collaboration has published measurements of several processes involving the π^0 meson, such as the $D^0 \to \pi^-\pi^+\pi^0$ decay [3] and the $B^0_{(s)} \to J/\psi\,\eta$ decays where the η meson decays to the $\pi^+\pi^-\pi^0$ final state [4]. However, the decay topologies considered in this work, $B \to h\pi^0$, where h denotes a charged or neutral hadron, present additional challenges in the LHCb environment. They suffer from a low π^0 meson reconstruction efficiency, which in the case of the $B^+ \to K^+\pi^0$ decay, results in an overall reconstruction efficiency of about 11%. Due to the lifetime of the h hadron, the decays considered lack a secondary vertex, a signature typically required by LHCb hadronic triggers. Altogether, these aspects result in low overall signal efficiencies and high combinatorial backgrounds.

A strategy for extracting $B^+ \to K^+\pi^0$ decays from the current LHCb data, along with techniques applicable to analyses of modes with similar topologies is presented. This analysis also provides a basis for the development of a dedicated inclusive software trigger for the next data-taking period, which can be used in future analyses of these channels. The study is performed with the 3.0 fb^{-1} data set recorded by the LHCb detector at centre-of-mass energies of 7 TeV and 8 TeV in 2011 and 2012, respectively.

2 Detector, data collection, and simulation

The LHCb detector [5] is a single-arm forward spectrometer covering the pseudorapidity range $2 < \eta < 5$, designed for the study of particles containing b or c quarks. The detector includes a high-precision tracking system consisting of a silicon-strip vertex detector surrounding the pp interaction region, a large-area silicon-strip detector located upstream of a dipole magnet with a bending power of about 4 Tm, and three stations of silicon-strip detectors and straw drift tubes placed downstream of the magnet. The tracking system provides a measurement of momentum, p, of charged particles with a relative uncertainty that varies from 0.5% at low momentum to 1.0% at 200 GeV/c. The minimum distance of a track to a primary vertex (PV), the impact parameter, is measured with a resolution of $(15 + 29/p_{\text{T}})\,\mu\text{m}$, where p_{T} is the component of p transverse to the

beam, in GeV/c. Different types of charged hadrons are distinguished using information from two ring-imaging Cherenkov detectors (RICH). Photons, electrons and hadrons are identified by a calorimeter system consisting of scintillating-pad and preshower detectors, an electromagnetic calorimeter (ECAL), and a hadronic calorimeter. Muons are identified by a system composed of alternating layers of iron and multiwire proportional chambers.

The trigger [6] consists of a hardware stage, based on information from the calorimeter and muon systems, followed by a software stage, which applies a full event reconstruction. The software trigger consists of many different algorithms (trigger lines) which run independently. Some trigger lines are inclusive, and serve a large range of the LHCb physics programme, while others are designed to trigger exclusively on specific decay modes. Events are said to be triggered on-signal (TOS) with respect to a particular trigger line when the constituents of a reconstructed signal candidate are sufficient to satisfy the requirements of that trigger [7]. Likewise, events are said to be triggered independent-of-signal (TIS) with respect to a given trigger line when the rest of the event is enough to satisfy that trigger's requirements.

With the exception of single-muon triggers, every software trigger line used during the 2011–2012 data-taking requires a reconstructed secondary vertex, hence $B^+ \to K^+\pi^0$ signal events cannot be TOS with respect to the software trigger. The presence of another secondary vertex in the event, independent of the signal, is then required for signal events to pass through this stage of the trigger. The trigger efficiencies are consequently very low, as this typically requires the presence of a second b hadron with enough transverse momentum and reconstructible daughters to satisfy the requirements of one of the trigger lines. In simulation, the overall trigger efficiencies are found to range from 5% to 11% over different data-taking periods and reconstruction strategies. These efficiencies are calculated as the fractions of triggered events in the total sample of simulated events that pass the cut-based selection described in Sect. 3. The dedicated software trigger line that is being developed is intended to recover a significant fraction of signal events which would otherwise be ignored at the data-taking stage.

In the simulation, pp collisions are generated using Pythia [8] with a specific LHCb configuration [9]. Decays of hadronic particles are described by EvtGen [10], in which final state radiation is generated using Photos [11]. The interaction of the generated particles with the detector and its response are implemented using the Geant4 toolkit [12] as described in Ref. [13].

3 Event selection

Reconstructed charged particles with a $p_{\rm T}$ greater than 250 MeV/c are used as K^+ candidates. They are required to be significantly displaced from the PV, and are distinguished from other charged particles using information from the RICH and calorimeter systems. Candidate π^0 mesons are reconstructed from neutral ECAL clusters. They are required to have $p_{\rm T}$ greater than 2.6 GeV/c, p greater than 10 GeV/c, and a reconstructed mass within the range $79.6 < m < 199.6\,{\rm MeV}/c^2$. In this kinematic range, the π^0 candidates

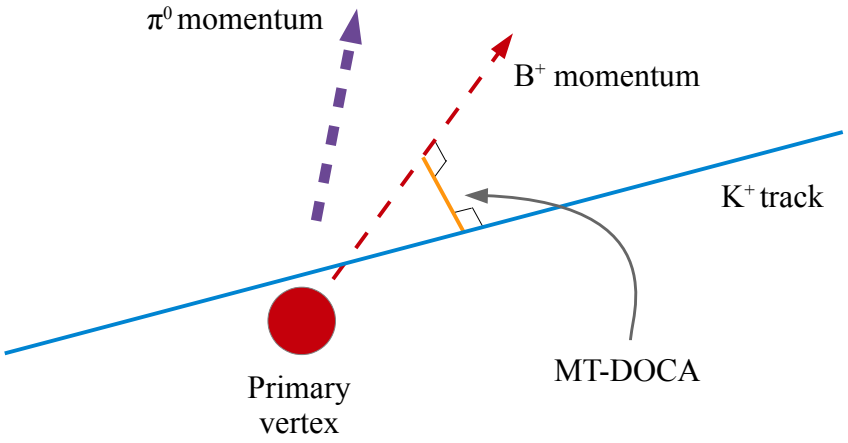

Figure 1: MT-DOCA and the reconstructed $B^+ \to K^+\pi^0$ decay topology.

are predominantly reconstructed from overlapping ECAL clusters, denoted as "merged" π^0 candidates. Candidates reconstructed from two separated ECAL clusters suffer from a large combinatorial background, mainly due to the abundance of low-energy ECAL clusters, and are not considered in this analysis. Overlapping particle showers produced in the ECAL by the π^0 mesons considered are transversely broader than those produced by single photons. The shower shape is therefore used to distinguish merged π^0 candidates from photon candidates. A track-matching algorithm is also used to reject charged clusters.

The momentum vector of the π^0 candidate is calculated using the energy and position information from the ECAL, and by taking the LHCb interaction point to be the origin. The four-momenta of the K^+ and π^0 candidates are added to form B^+ candidates. Each B^+ candidate is required to have a $p_{\rm T}$ greater than $1.5\,{\rm GeV}/c$, and a reconstructed mass within the range $4.0 < m < 6.0\,{\rm GeV}/c^2$. A trajectory is made from the PV closest to the daughter K^+ candidate, along the direction of the reconstructed B^+ candidate momentum. The variable called mother-trajectory distance-of-closest-approach (MT-DOCA) is the DOCA between the K^+ candidate and this trajectory. An illustration of the geometry involved is shown in Fig. 1. This variable is motivated by the significant displacement of the signal B^+ from its PV, and is designed to provide some quantitative measure of the decay position in the absence of a reconstructed decay vertex. For well-reconstructed signal events, the MT-DOCA is small, whereas the distribution of random combinations of final-state particles has a tail at large values. A χ^2 for the MT-DOCA is constructed using the covariance matrix of the reconstructed PV, and is shown in Fig. 2. In some cases, the K^+ meson from a signal decay is associated with the wrong PV. These signal events resemble the background, as can be see in Fig. 2, but the effect on the performance is small. The $\chi^2_{\text{MT-DOCA}}$ is required to be less than 10 for B^+ candidates reconstructed from 2011 data, and less than 9 for those reconstructed from 2012 data. The requirements for the two data-taking periods are optimised separately to allow for different background levels at different centre-of-mass energies, though the difference in performance of the requirements is ultimately negligible.

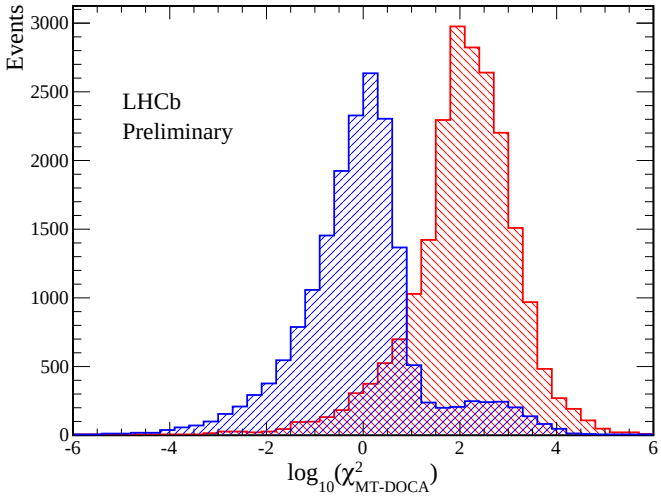

Figure 2: Signal and background distributions of $\log_{10}(\chi^2_{\text{MT-DOCA}})$ for 2012 conditions. The signal contribution from simulated data is shown in hatched blue, and the background contribution from mass sidebands in the recorded data is shown in hatched red.

Variables characterizing how well-isolated a candidate is from other tracks in the event are also calculated. Vertex isolation variables are calculated by combining another track in the event with the K^+ candidate to form a two-track secondary vertex. This procedure is performed for all tracks in the event. The multiplicity of two-track secondary vertices with $\chi^2_{\text{vtx}} < 9$ is recorded as the variable $V_{\text{Mult.}}$, where χ^2_{vtx} is the χ^2 of the vertex fit. Of these vertices, the one with the smallest χ^2_{vtx} is built on to form a four-track vertex. The two additional tracks used are those that result in the smallest χ^2_{vtx} after being added to the vertex. The variable $\min(\Delta\chi^2_{\text{vtx}})$ is then given by the change in the χ^2_{vtx} upon adding these two tracks. Candidates reconstructed from 2011 data are required to have a $V_{\text{Mult.}}$ fewer than 8, and those reconstructed from 2012 data are required to have a $V_{\text{Mult.}}$ fewer than 6. The requirements for the two data-taking periods are optimised separately to allow for different performance at different centre-of-mass energies.

The p_{T} asymmetry of the reconstructed B^+ candidate is defined as

$$\mathcal{A}(p_{\text{T}}) = \frac{p_{\text{T}B} - p_{\text{T}\,\text{cone}}}{p_{\text{T}B} + p_{\text{T}\,\text{cone}}}, \tag{1}$$

where $p_{\text{T}B}$ is the transverse momentum of the reconstructed B^+ signal candidate, and $p_{\text{T}\,\text{cone}}$ is the magnitude of the vector sum of the transverse momenta of the charged particles near the reconstructed B^+ candidate. It is used to isolate the reconstructed candidate from nearby tracks. To determine whether a track is "near" the signal candidate, the quantity $\Delta R = \sqrt{(\Delta\phi)^2 + (\Delta\eta)^2}$ is required not to exceed 1.2, where $\Delta\phi$ is the difference between the azimuthal angle of the momentum of the reconstructed candidate and the track, and $\Delta\eta$ is the difference between their pseudorapidities. The cone size, $\Delta R = 1.2$, is optimised using simulated data for the signal, and a subsample of experimental data for the background.

In order to maximise the sensitivity, a multivariate analysis is developed using a boosted decision tree (BDT) [14, 15] classifier. Among the event classification variables are the isolation variables $\mathcal{A}(p_{\rm T})$, $V_{\rm Mult.}$, and $\min(\Delta\chi^2_{\rm vtx})$, which depend on the multiplicity of non-signal tracks in the event. To ensure that the simulated $B^+ \to K^+\pi^0$ distributions of these variables are correct, event weights are generated from the ratios of these distributions between experimental and simulated $B^0 \to K^+\pi^-$ events. The rest of the event classification variables are the p and $p_{\rm T}$ of the B^+, K^+, and π^0 candidates, the pseudorapidity of the B^+ candidate, the $\chi^2_{\rm IP}$ of the K^+ candidate, and the $\chi^2_{\text{MT-DOCA}}$. The $\chi^2_{\rm IP}$ is defined as the difference in χ^2 of a given PV reconstructed with and without the considered track. The multivariate classifier is trained and tested using experimental data to represent the background, and simulated $B^+ \to K^+\pi^0$ data that are corrected using the event weights. The optimal cut value of the classifier response variable is found for the data set by maximising the figure of merit $N_S/\sqrt{N_S + N_B}$, where N_S is the number of signal events and N_B is the number of background events. While optimal, this requirement has a very low signal efficiency, roughly 7%, as a consequence of the low trigger efficiency and enormous combinatorial background. The total efficiency, accounting for all geometric acceptance, trigger, and selection requirements is of the order 3×10^{-5}.

4 Results

The mass distribution of reconstructed candidates, after all selection requirements, is shown in Fig. 3. To extract the number of signal events, we fit a model to this distribution which consists of an exponential function for the combinatorial background; the tail of a Gaussian function for additional background in the low-mass region; and the sum of two Crystal Ball functions [16] for the signal, to account for the tails on both sides of the signal peak. The Crystal Ball functions share a common mean and width, and their tail shapes are taken from simulation. The background remaining in the final selection consists primarily of partially reconstructed $B \to K^+\pi^0 X$ decays, or B^+ candidates reconstructed with misidentified π^0 candidates. Several exclusive decay modes, including $B \to K^*\pi^0$, $B \to K^+\rho$, and $B \to K^*\gamma$ are also considered and are found to make negligible contributions in the signal region. The shape of the combinatorial background is determined from a fit to the upper sideband. Normalisations of the individual components are allowed to float in the fit, as well as the means and widths of the signal and low-mass background shapes.

A signal yield of 72 ± 26 candidates is found. The statistical significance of the signal is determined from the change in the fit likelihood, with and without a signal component, to be 3.7σ. The signal width of $99 \pm 38\,\text{MeV}$ is consistent with the expected resolution from simulation, which is estimated to be $95 \pm 4\,\text{MeV}$. Several variations of the fit are performed with different shapes modelling the low-mass background. Variations are also performed with and without the signal width fixed from simulation, and with the signal mean fixed to the known value of the B^+ mass. All variations are found to be compatible with the fit shown here, and a systematic uncertainty of the signal yield due to the choice of fit model is estimated to be 10 events.

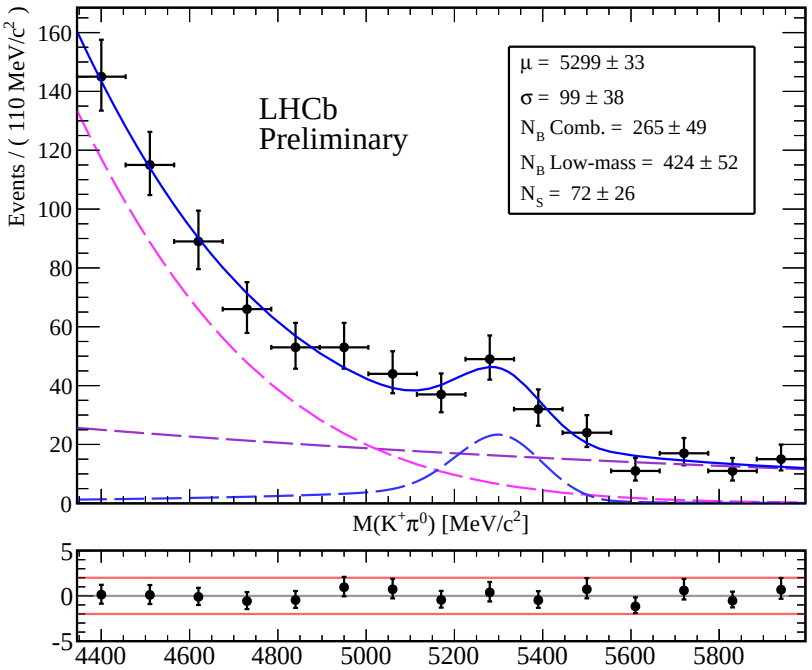

Figure 3: Mass distribution of the reconstructed candidates, selected from the entire data set. The data are drawn as black points. The fit to the B^+ reconstructed mass is drawn as a solid blue line. The signal component is drawn in dashed blue, the combinatorial background is drawn in dashed purple, and the low-mass background is drawn in dashed magenta.

5 Prospects for 2015 and beyond

A rough estimate of the prospects for this channel in the next data-taking period is made by taking into account expected improvements due to a dedicated software trigger line ($\times$3–5), the increased $b\bar{b}$ cross section at 13 TeV($\times$2), and the potentially increased overall offline analysis efficiency ($\times$5). The software stage of the trigger that would be improved by a dedicated trigger line is estimated from simulation to be about 16% efficient during the 2011–2012 data-taking, after offline reconstruction. This efficiency is typically above 75% for b-hadron decays to two charged particles [6], so an improvement of at least a factor of 3 is not unrealistic. In order to assess possible improvements in the offline analysis efficiency due to the enhanced yield as a result of the improved trigger, an estimate of the expected combinatorial background level during the next data-taking period is required. The background is assumed to be dominated by generic $b\bar{b}$ events, the cross section for which scales linearly with centre-of-mass energy. This assumption is supported by the absence of significant contributions from exclusive partially reconstructed modes whose rate could potentially increase with the future dedicated trigger. A data sample representing the expected effect on the background level of a factor 5 increase in the total offline efficiency is selected from the 2011–2012 data by loosening the requirement on the multivariate classifier. This, together with appropriately scaled simulated signal events, is

used to estimate the possible signal significance with this modified selection. We estimate a signal yield of 700–1100 events in $1\,\text{fb}^{-1}$ of integrated luminosity gathered in the next data-taking period, with an uncertainty of about 100 events, dominated by the background yield. This neglects other sources of improvements such as increased identification and reconstruction efficiencies of π^0 mesons, and a reoptimised and retrained multivariate classifier.

6 Conclusions

A study of the decay $B^+ \to K^+\pi^0$ is performed with the LHCb 2011–2012 data set. Despite a low trigger efficiency, and a very low selection efficiency after suppressing the combinatorial background, evidence for a signal is found for the first time at a hadron collider, using candidates reconstructed with a merged π^0 candidate. With a dedicated software trigger line in place, measurements in this decay channel will be possible in the next data-taking period at an estimated level of 10% precision with $1\,\text{fb}^{-1}$ of data.

Motivated by the results of this study, a software trigger line is being developed using merged π^0 candidates from the hardware stage of the trigger to reconstruct signal candidates. The goal driving the development of the trigger is to obtain as much efficiency in the $B^+ \to K^+\pi^0$ channel as possible, with the potential to extend it to other modes in this class of decay channels.

References

[1] Heavy Flavor Averaging Group, Y. Amhis *et al.*, *Averages of b-hadron, c-hadron, and τ-lepton properties as of early 2012*, arXiv:1207.1158, updated results and plots available at http://www.slac.stanford.edu/xorg/hfag/.

[2] LHCb collaboration, R. Aaij *et al.*, *First evidence of direct CP violation in charmless two-body decays of B_s^0 mesons*, Phys. Rev. Lett. **108** (2012) 201601, arXiv:1202.6251.

[3] LHCb collaboration, R. Aaij *et al.*, *Search for CP violation in $D^0 \to \pi^-\pi^+\pi^0$ decays with the energy test*, Phys. Lett. **B740** (2015) 158, arXiv:1410.4170.

[4] LHCb collaboration, R. Aaij *et al.*, *Study of η–η' mixing from measurement of $B^0_{(s)} \to J/\psi\eta^{(\prime)}$ decay rates*, JHEP **01** (2015) 024, arXiv:1411.0943.

[5] LHCb collaboration, A. A. Alves Jr. *et al.*, *The LHCb detector at the LHC*, JINST **3** (2008) S08005.

[6] R. Aaij *et al.*, *The LHCb trigger and its performance in 2011*, JINST **8** (2013) P04022, arXiv:1211.3055.

[7] A. Puig, *The LHCb trigger in 2011 and 2012*, Tech. Rep. LHCb-PUB-2014-046. CERN-LHCb-PUB-2014-046, CERN, Geneva, Nov, 2014.

[8] T. Sjöstrand, S. Mrenna, and P. Skands, *PYTHIA 6.4 physics and manual*, JHEP **05** (2006) 026, arXiv:hep-ph/0603175; T. Sjöstrand, S. Mrenna, and P. Skands, *A brief introduction to PYTHIA 8.1*, Comput. Phys. Commun. **178** (2008) 852, arXiv:0710.3820.

[9] I. Belyaev *et al.*, *Handling of the generation of primary events in* Gauss*, the LHCb simulation framework*, Nuclear Science Symposium Conference Record (NSS/MIC) **IEEE** (2010) 1155.

[10] D. J. Lange, *The EvtGen particle decay simulation package*, Nucl. Instrum. Meth. **A462** (2001) 152.

[11] P. Golonka and Z. Was, *PHOTOS Monte Carlo: a precision tool for QED corrections in Z and W decays*, Eur. Phys. J. **C45** (2006) 97, arXiv:hep-ph/0506026.

[12] Geant4 collaboration, J. Allison *et al.*, *Geant4 developments and applications*, IEEE Trans. Nucl. Sci. **53** (2006) 270; Geant4 collaboration, S. Agostinelli *et al.*, *Geant4: a simulation toolkit*, Nucl. Instrum. Meth. **A506** (2003) 250.

[13] M. Clemencic *et al.*, *The LHCb simulation application,* Gauss*: design, evolution and experience*, J. Phys. Conf. Ser. **331** (2011) 032023.

[14] L. Breiman, J. H. Friedman, R. A. Olshen, and C. J. Stone, *Classification and regression trees*, Wadsworth international group, Belmont, California, USA, 1984.

[15] R. E. Schapire and Y. Freund, *A decision-theoretic generalization of on-line learning and an application to boosting*, Jour. Comp. and Syst. Sc. **55** (1997) 119.

[16] T. Skwarnicki, *A study of the radiative cascade transitions between the Upsilon-prime and Upsilon resonances*, PhD thesis, Institute of Nuclear Physics, Krakow, 1986, DESY-F31-86-02.

A Additional figures

Figs. 4 and 5 show the reconstructed B mass from simulated data of $B^+ \to K^+\pi^0$ decays that pass the selection requirements, and the response of the multivariate classifier, respectively.

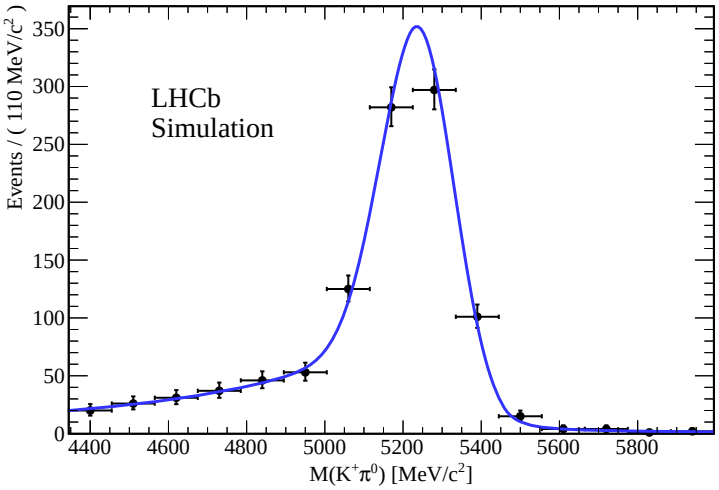

Figure 4: Reconstructed B^+ mass distribution from simulated data of $B^+ \to K^+\pi^0$ decays that pass the selection requirements.

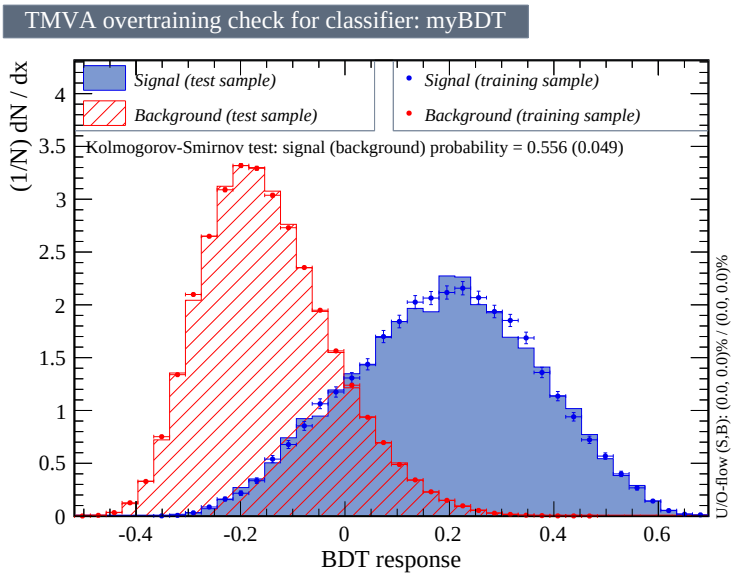

Figure 5: Distribution of the classifier response variable. The signal contribution from simulated data is shown in solid blue, and the background contribution from experimental data is shown in hatched red.